Analysis of the August 2017 Eclipse's Effect on Radio Wave Propagation Employing a Raytrace Algorithm

M.L. Moses[1], G.D. Earle[1], L. Kordella[1], M. Ruohoniemi [1], K. Sterne[1], J. Vega[2], N.A. Frissell[2]

[1]Virginia Tech, [2]New Jersey Institute of Technology

Abstract

The total solar eclipse over the continental United States on August 21, 2017 offered a unique opportunity to study the dependence of the ionospheric density and morphology on incident solar radiation. Unique responses may be witnessed during eclipses, including changes in radio frequency (RF) propagation at high frequency (HF). Such changes in RF propagation were observed by the Super Dual Auroral Radar Network (SuperDARN) radars in Christmas Valley, Oregon and in Fort Hayes, Kansas during the past summer's eclipse. At each site, the westward looking radar observed an increase in slant range of the backscattered signal during the eclipse onset followed by a decrease after totality. In order to investigate the underlying processes governing the ionospheric response to the eclipse, we employ the HF propagation toolbox (PHaRLAP), created by Dr. Manuel Cervera, to simulate SuperDARN data for different models of the eclipsed ionosphere. By invoking different hypotheses and comparing simulated results to SuperDARN measurements we can study the underlying processes governing the ionosphere and improve our model of the F-Region responses to an eclipse.

Introduction

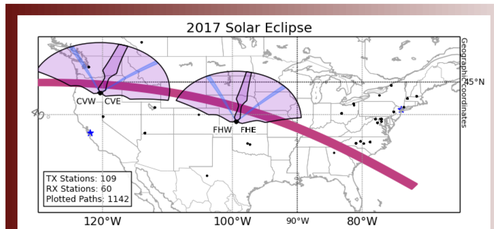

Figure 1. Eclipse path (maroon) crossed SuperDARN fields of view (violet) and camping beams (blue).

SuperDARN Operations

- The Christmas Valley and Fort Hayes SuperDARN radars ran at ~10.5 MHz in every-other-beam mode on eclipse day order to maximize the temporal resolution of data from the camping beams (Fig. 1).

SuperDARN Data

- The westward-looking radars at Christmas Valley and Fort Hayes observed distinct variations in ionospheric propagation during the eclipse . Hence, the focus of this poster is on the data from the camping beams of the Christmas Valley West (CVW) and Fort Hayes West (FHW) radars.

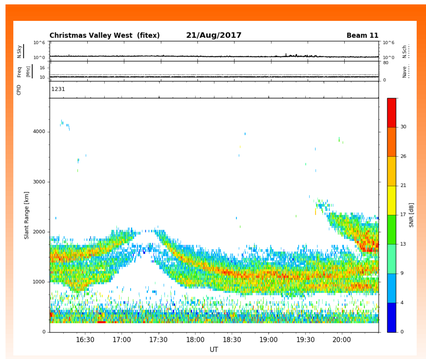

Figure 2. Christmas Valley West beam 11 Range-Time-Intensity plot.

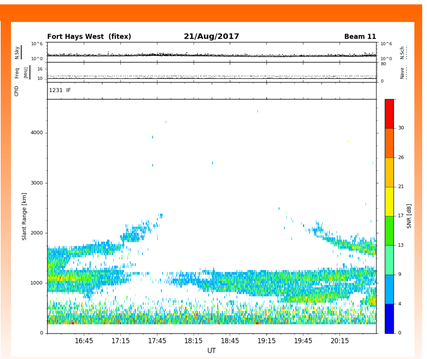

Figure 3. Fort Hayes West beam 11 Range-Time-Intensity plot.

- Both the CVW and FHW SuperDARN sites show an increase in slant range associated with the eclipse. However, the responses' durations and magnitudes differ.
- Why do the data from the two SuperDARN sites show such stark differences?

Hypothesis

- The geometry of the eclipsed region is different for the two sites so the transport mechanisms that replenish the plasma in the eclipsed regions are different.

Eclipse Geometry

Raytrace Model

- Using our raytrace model we selected reflection points (Figure 4 and Table 1) for each site to investigate these differences.

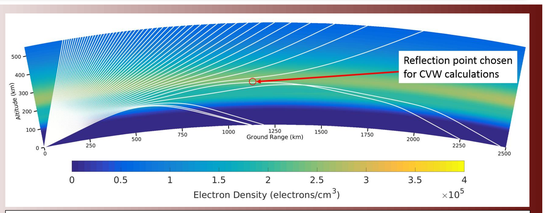

Figure 4. Raytrace of CVW beam 11 during eclipse.

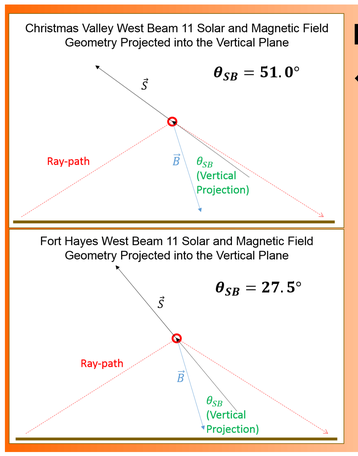

Flux Tube Geometry

- Investigation of the relative orientation of geomagnetic field ($\vec{B}$) to the vector connecting the sun to the reflection point ($\vec{S}$) revealed that the flux tube and the sun are closely aligned at Fort Hayes reflection point while the flux tube and sun are less closely aligned at the Christmas Valley reflection point (Figures 5 and 6 and Table 1).

Figure 5 (upper) and Figure 6 (lower). Vertical profile of the magnetic field at and the solar location relative to the reflection point of each SuperDARN site.

Eclipse Attenuation Model

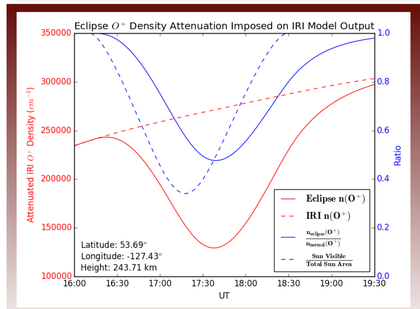

Figure 7. Modeled Eclipse Response for the Reflection Point of the CVW Beam

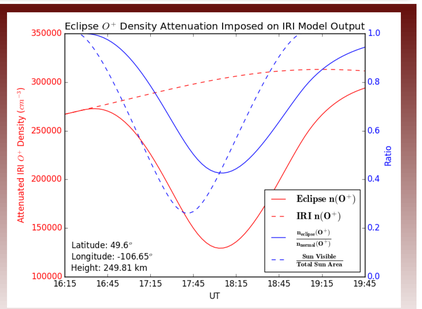

Figure 8. Modeled Eclipse Response for the Reflection Point of the FHW Beam

Ionization and Recombination Model

- The uneclipsed and eclipsed ion densities for each point were calculated using the model for F-region ionization and recombination given in (*Banks and Kockarts, 1973*). Then, the corresponding plasma attenuation functions, shown in Figures 7 and 8, were calculated by dividing the eclipsed ion densities by the uneclipsed ion densities.

Results

- This eclipse model was applied to estimate the velocities of plasma diffusion into each region at the time of maximum plasma depletion.

Christmas Valley Reflection Point *Latitude: 53.69°* *Longitude: -127.43°* *Altitude: 243.71 km* *Universal Time: 17:39 UT*	$\lvert\hat{S}\cdot\hat{B}\rvert$	~0.6
	$V_{\parallel}\ diffusion$	~711.3 m/s
	$V_{\perp}\ diffusion$	~3.3x10^{-7} m/s
	HWM velocity	~7.5 m/s
	ExB velocity	~200 m/s
	$\parallel diffusion$ time	~7 minutes
	ExB time	~42 minutes
Fort Hayes Reflection Point *Latitude: 49.6°* *Longitude: -106.65°* *Altitude: 249.81 km* *Universal Time: 18:06 UT*	$\lvert\hat{S}\cdot\hat{B}\rvert$	~0.9
	$V_{\parallel}\ diffusion$	~1050 m/s
	$V_{\perp}\ diffusion$	~7.8x10^{-8} m/s
	HWM velocity	~11.2 m/s
	ExB velocity	~200 m/s
	$\parallel diffusion$ timescale	~ 5 minutes
	ExB timescale	~42 minutes

Table 1. Summary of solar geometry and plasma transport velocities and timescales.

- The results in Table 1 indicate that parallel diffusion is the quickest mechanism for plasma transport to the depleted eclipsed regions.
- At the Fort Hayes (FH) point, the close alignment of the sun and flux tube during the eclipse suggests that the plasma along the flux tube will be depleted. Hence, there is less high altitude plasma available to refill the given region at FH than there is at Christmas Valley (CV).
- Thus, diffusion of higher altitude plasma into the depleted eclipsed region at CV leads to the symmetry between the onset and recovery phases in the CVW data. However, the region at FH does not recover as quickly because there is less high altitude plasma available to refill the depleted region, which leads to the asymmetry in the FHW data.

Conclusions and Future Work

- Our results suggest that parallel diffusion is the dominant mechanism for replenishing the depleted plasma in the eclipsed region. The second most efficient mechanism is ExB drift.
- The alignment of the flux tube relative to the sun at each site during the eclipse is likely the cause of the differences in the CVW and FHW data.
- More extensive modeling is needed to verify our hypothesis; however, the estimates presented here indicate what the dominant factors should be when modeled in SAMI3.

References and Acknowledgments

P. Banks and G. Kockarts, *Aeronomy*. New York, New York: Academic Press Inc., 1973.

M. C. Kelly, *The Earth's Ionosphere: Plasma Physics and Electrodynamics*. San Diego, California: Academic Press, Inc., 1989.

F. F. Chen, *Introduction to Plasma Physics and Controlled Fusion*, Third ed.: Springer International Publishing, 2016.

This work was supported by NSF Grant # AGS-1552188 and NASA Grant #NNX17AH70G.

The results presented in this poster were obtained using the HF propagation toolbox, PHaRLAP, created by Dr. Manuel Cervera, Defence Science and Technology Organisation, Australia (manuel.cervera@dsto.defence.gov.au). This toolbox is available by request from its author.

Joe Huba and Doug Drob, for SAMI3 output files used in raytrace simulation.

Drew Compston: "International Geomagnetic Reference Field (IGRF) Model" (Matlab code)

David Eagle: "A MATLAB Script for Predicting Solar Eclipses"

We acknowledge the use of the Free Open Source Software projects used in this analysis: Ubuntu Linux, Python, iPython, matplotlib, NumPy, SciPy, scikit-learn,Davitpy, and others.

Contact: magda14@vt.edu

CEDAR 2018